Global **A**dvances in **M**ultidisciplinary **A**pplications in **N**ext-Gen **A**nd **M**odern Technologies (**GAMANAM)**
Volume 1, Issue 1, January 2025, Pp: 16-22
© 2025, SPMVV All Rights Reserved

Research Paper

Unbalance Voltage in LV Micro grid Compensated by Using ANFIS and PI-based Add-on Controller

[1]M Pallavi, [2]K Shalini, [3*]D Narmitha, [4]G. Rekha

[1,2,3]Associate professor, Department of Electrical and Electronics Engineering, School of Engineering and Technology, Sri Padmavati Mahila Visvavidyalayam, Tirupati*
[4]Associate professor, Department of Computer Science and Engineering, School of Engineering and Technology, Sri Padmavati Mahila Visvavidyalayam, Tirupati

**Corresponding Author(s): dama.narmitha@gmail.com*

Received: 02/11/2024, Revised: 29/11/2024, Accepted: 26/12/2024 Published: 12/01/2025

Abstract: Several distributed aging voltage source converters (VSCs) are used in a low voltage microgrid (LVMG) to balance the voltage compensation. This paper outlines the use of an ANFIS and a PI-based add-on controller. The issue is further misrepresented by the nearness of the unbalance load at the purpose of the normal coupling (PCC). To lessen the negative consequences of an unbalanced load, the standard VSC control has been enhanced with an ANFIS add-on regarding the control circle. The additional controller in this case adjusts the reference current additions in accordance with the voltage imbalance factor. Additional controller's reference current increases are added to voltage control circle's yield to set updated reference current for inward current control circle. The planned control calculation has been approved based on the broad recreation results and test permission.

Keywords: ANFIS and PI based Add-on Controller, VSC Converter, VSC based Low Voltage Microgrid (LVMG).

1 Introduction

Globally, microgrids are gaining popularity due to their capacity to function autonomously in an islanding mode. Additionally, the microgrid makes it possible to strategically utilize easily accessible renewable energy sources (RES) to serve remote areas with slow network access. In this sense, both the framework tied mode and the off matrix (islanded) mode must be used by the microgrid. The network voltage serves as the reference for DG interacting VSCs in lattice linked mode, and there is little chance of an inside collision between different VSCs. However, in the islanded way of activity, the unique VSCs should have been managed so that each connected VSC shares the heap request in proportion to its unique rating. [1]– [4]. As a result, a micro grid's VSCs can be managed in two different ways: either all at once via a dedicated correspondence channel, or one at a time via hang control, which may call for a low transfer speed correspondence channel or none at all [5]–[7]. Nonetheless, compliance with such a control strategy is required.

Correspondence channel and eliminates the important focal points of the micro grid's playback and fitting capabilities. To counteract the detrimental consequences of a progressively shifting imbalance load, a unique add-with-respect to controller ANFIS has been proposed in the work. Versatile neuro fluffy derivation frameworks (ANFIS) are incredibly powerful since they can handle vulnerabilities similar to fluffy frameworks and benefit from processes similar to neural frameworks. [8]- [12]. In this way, the ANFIS controller adaptively handles the problem of settling as much as feasible under dynamic situations. To control the imbalance voltage factor, the suggested solution entails deleting the negative grouping voltage section. The negative arrangement voltage part is pushed to the ANFIS controller, resulting in equal unbalanced current. The internal current control circles' reference current is adjusted by addition the imbalance current segment to the yield of the external voltage control circles.

2 System Overview

In the event that a simple lattice is not there, the micro grid's primary goal is to sustain the distributed neighborhood load. Accordingly, unlike the primary matrix, the microgrid must be limited to a much smaller land region and have its own age, transmission, and dissemination mechanism.

This is an open access article under the CC BY-NC-ND license (http://creativecommons.org/licenses/by-nc-nd/4.0/)

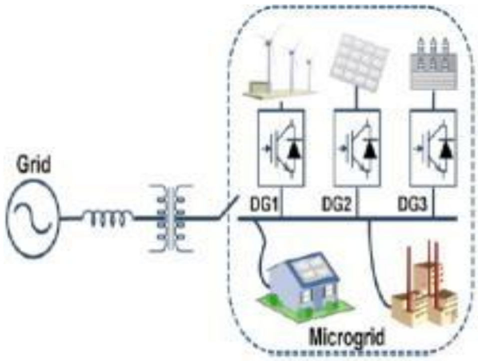

Figure 1: Micro grid Connected with Hybrid solar and Wind Energy

A typical microgrid consists of multiple parallel DGs connected by power gadget-based VSCs to form an AC arrangement. Renewable energy sources, including solar panels, wind turbines, and a small backup battery, are used by the microgrid control system shown in Figure 1. The heap may consist of three stages in addition to a single stage with an uneven profile and both modified. Given that the microgrid is essentially an inactive framework, any variation in the burden circumstances will have an adverse influence on the voltage design. In this way, an imbalance in the inventory voltage profile may result from any kind of unbalance burden. In this way, it is necessary in parallel so that they can give imbalance current in response to burden requests with no deviation from the optimum corrected sinusoidal voltage profile. All concurrently associated DGs are able to function as a typical hang control because there is no discernible looping current, and they are instructed to share the heap request based on their rating.

3 Monitoring Proposal

The point by point portrayal of the general framework with suggested method of control has surfaced in Figure 2. For the suggested microgrid, three-stage frameworks with coasting unbiased have been taken into consideration. The microgrids small size and unbalanced load make it challenging to maintain the optimal configuration of PCC inventory voltage through three-stage adjusted voltages. In this way, the inventory voltage will unquestionably comprise all three grouping components. (The sequence includes positive, negative, and zero sequences). None of the zero succession components have been taken into consideration due to the nonpartisan wire's nonattendance. The negative succession voltage has been eliminated through voltage imbalance pay, and the negative portion is further restricted using an ANFIS combined add to the controller.

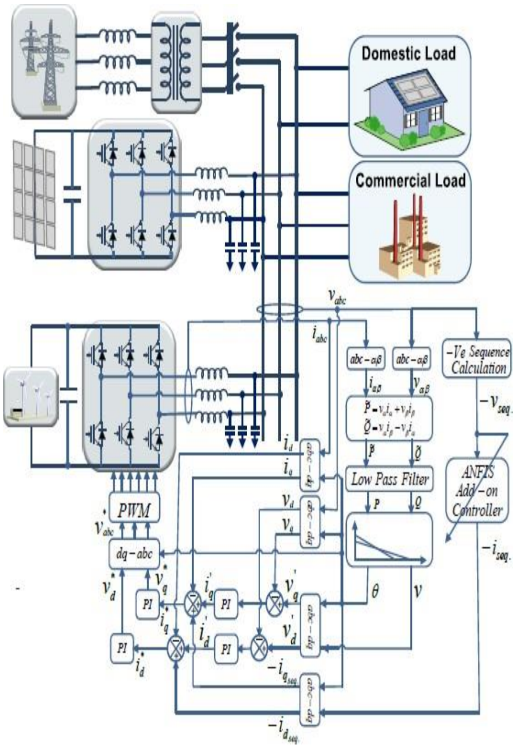

Figure 2: Description of Microgrid Control

3.1 Extracting voltage in a negative sequence

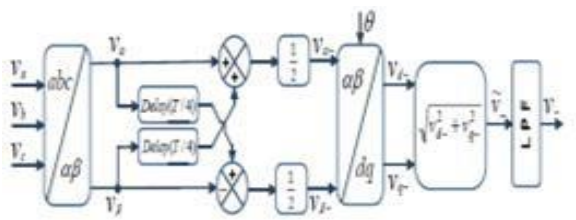

Figure 3: Voltage Extraction in Negative sequence

One of the most difficult concepts to comprehend is the power framework system's unbalance mystery. The balanced segments technique is a widely used method to identify asymmetry or twisting in framework voltages. Even part technique faces issues this method uses phasors instead of time space signals and necessitates a modification of the turning space vector to extract the sequence segment. A few modifications have been made to represent the imbalance voltages in a scientific manner. The most common uses for Clarke and Park's modifications are as voltage guidelines and regulate usage. However, in the event of an imbalance. In the rearranged voltage setup, the second request song is played in the negative succession segment. As a result, the modifications made by Clarke and Park should be classed in order to remove the negative arrangement section for the purpose of voltage guidelines. Without the use of an impartial wire, the voltage conditions of a three-stage system is expressed as follows by the positive and negative arrangement components.

$$v_a = v_p.\cos(\omega t) + v_n.\cos(-\omega t) \quad (1)$$

$$v_b = v_p.\cos\left(\omega t - \frac{2\pi}{3}\right) + v_n.\cos\left(-\omega t + \frac{2\pi}{3}\right) \quad (2)$$

$$v_c = v_p.\cos\left(\omega t + \frac{2\pi}{3}\right) + v_n.\cos\left(-\omega t - \frac{2\pi}{3}\right) \quad (3)$$

$$v_{\alpha} = v_n.\cos(\omega t) + v_p.\cos(\omega t) = v_{\alpha-} + v_{\alpha+} \quad (4)$$

$$v_{\beta} = v_p.\sin(\omega t) - v_n.\sin(\omega t) = v_{\beta+} + v_{\beta-} \quad (5)$$

The positive sequence components are represented by $v\alpha+$ and $v\beta+$, while the negative sequence components are represented by $v\alpha-$ and $v\beta-$. The equations (4) and (5) can be expressed as follows, as long as the symmetrical components remain unchanged for a minimum of 25% of a cycle.

$$v_{\alpha+}(t) = \frac{1}{2}\left(v_{\propto}(t) - v_{\beta}\left(t - \frac{T}{4}\right)\right) \quad (6)$$

$$v_{\beta+}(t) = \frac{1}{2}\left(v_{\propto}(t) - v_{\beta}(t)\right) \quad (7)$$

$$v_{\alpha-}(t) = \frac{1}{2}\left(v_{\propto}(t) - v_{\beta}\left(t - \frac{T}{4}\right)\right) \quad (8)$$

$$v_{\beta-}(t) = \frac{1}{2}\left(v_{\propto}\left(t - \frac{T}{4}\right) - v_{\beta}(t)\right) \quad (9)$$

The negative sequence components from equations (8) and (9) are transformed into a rotating reference frame using Park's transformation, which is subsequently utilized to extract the relevant component.

3.2 Building an Add-on Controller Using ANFIS as the Model

By keeping the negative succession voltage at zero, the suggested controller will allow for an unbalanced load to be promoted and an adjusted three-stage voltage configuration at PCC. Situations with uneven dynamic loads may cause significant fluctuations in the negative arrangement voltage. It requires a lot of work to determine the appropriate additions of a normal PI controller in order to correct voltage imbalance. After that, an ANFIS that is planned in connection to the controller is put together, and it adjusts its baseline rises according to the operational conditions. An ANFIS controller based on the Takagi-Kang-Sugeno fluffy model with a 1:3:3:3:1 design, single info, and only one yield was applied. The recommended ANFIS engineering was taken from our earlier distribution. [22]. Accordingly, the suggested ANFIS controller consists of five layers, the first of which is referred to as the fuzzification layer and which uses three enrollment capacities to fuzzily the negative arrangement voltage. Here, the coefficients of the conditions speaking to are used in conjunction with trapezoidal and triangular capabilities.

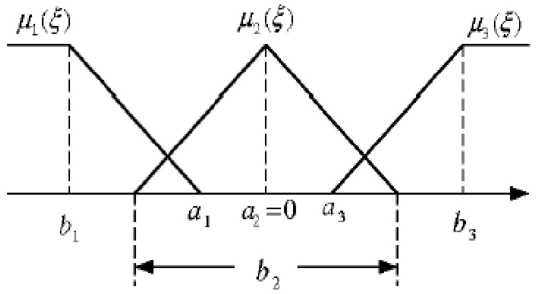

Figure 4: Uncertainty in membership functions

As input changes, these functions are updated continually. The mathematical expression for the trapezoidal functions displayed in Figure. 4 is

$$\mu_{A_1}(\xi) = \begin{cases} 1 & \xi \le b_1 \\ \frac{\xi - a_1}{b_1 - a_1} & b_1 < \xi < a_1 \\ 0 & \xi \ge a_1 \end{cases} \quad (10)$$

$$\mu_{A_1}(\xi) = \begin{cases} 1 - \frac{\xi - a_3}{b_3 - a_3} & |\xi - a_2| \le 0.5 b_2 \\ 0 & |\xi - a_2| \ge 0.5 b_2 \end{cases} \quad (11)$$

$$\mu_{A_3}(\xi) = \begin{cases} 0 & \xi \le a_3 \\ \frac{\xi - a_3}{b_3 - a_3} & a_3 < \xi < b_3 \\ 1 & \xi \ge b_3 \end{cases} \quad (12)$$

When an error occurs, the estimation of parameters a_i and b_i alters accordingly, generating the phonetic value of each enrollment task as needed. This layer's parameters are referred to as precondition or reason parameters. Since there is only one contribution at each hub. The duplication layer transfers the sign to the third layer, which contains standardized signs. Diagram. Alternatively referred to as the following layer, the fourth layer is where each parameter is updated anew in light of the variances. The fifth layer functions as a yield layer by effectively summarizing all of the signals originating from the several hubs in the fourth layer. Figure 5 shows the ANFIS design in its entirety.

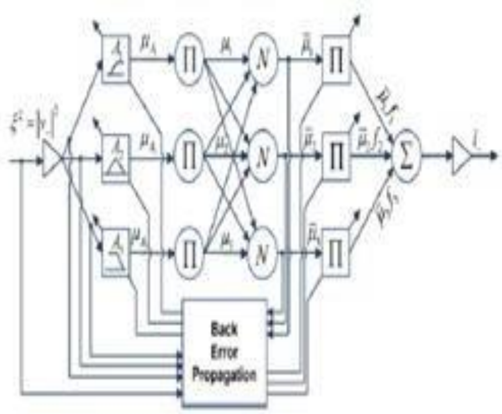

Figure 5: Architecture of ANFIS

3.3 Training of ANFIS Architecture

In the same way that the negative arrangement voltage portion has been seen as a mistake, ANFIS has been adjusted to minimize this mistake. In order to refresh the loads, mistakes are transferred from the yield layer to the inclusion layer using the angle plunge approach. Back propagation is the term used to describe this process of replenishing the loads. The tuning procedure involves two layers: First layer pre-condition tuning and fourth layer subsequent tuning. The square of the negative succession voltage segment is the definition of the target work.

$$\xi^2 = ((0 - v\_)^2 = |v\_|^2 \quad (13)$$

(a). **Adjustment of precondition parameters:**

It's crucial to keep in mind that updating the fuzzy membership functions requires changing the Precondition parameters. The error function and the Precondition parameter change are connected to one another as

$$\Delta a_{A1} = -\eta \frac{\partial \xi^2}{\partial a_{A1}} \quad i = 1,2,3 \quad (14)$$

The learning rate is represented by η. The parameter's updated value is expressed as follows:

$$a_{A1}(n+1) = a_{A1}(n) + \Delta a_{A1} \quad i = 1,2,3 \quad (15)$$

Or

$$a_{A1}(n+1) = a_{A1}(n) - \eta \frac{\partial \xi^2}{\partial a_{A1}} \quad i = 1,2,3 \quad (16)$$

Using differentiation chain rule, the following formula can be used to find the partial derivative term in equation (16).

$$\frac{\partial \xi^2}{\partial a_{A1}} = \frac{\partial \xi^2}{\partial V\_}.\frac{\partial V\_}{\partial i\_}.\frac{\partial i\_}{\partial \overline{\mu_1}}.\frac{\partial \overline{\mu_1}}{\partial \mu_{A1}}.\frac{\partial \mu_{A1}}{\partial a_{A1}} \quad (17)$$

Where

$$\frac{\partial \xi^2}{\partial V\_} = -2(0 - V\_) = -2\xi \quad (18)$$

$$\frac{\partial V\_}{\partial i\_} = J \quad (19)$$

$$i\_ = \overline{\mu_1}.f_1 + \overline{\mu_2}.f_2 + \overline{\mu_3}.f_3 \Rightarrow \frac{\partial i\_}{\partial \overline{\mu_1}} = f_1; \quad (20)$$

$$\overline{\mu_1} = \frac{\mu_{A1}}{\mu_{A1} + \mu_{A2} + \mu_{A3}} \Rightarrow \frac{\partial \overline{\mu_1}}{\partial \mu_{A1}} = \frac{(\overline{\mu_2} + \overline{\mu_3})}{\mu_{A1} + \mu_{A2} + \mu_{A3}} \quad (21)$$

$$\mu_{A1} = \frac{\xi - a_{A1}}{b_{A1} - a_{A1}} \Rightarrow \frac{\partial \mu_{A1}}{\partial a_{A1}} = \frac{\mu_{A1} - 1}{b_{A1} - a_{A1}}; \quad (22)$$

The Jacobean matrix, denoted by J in this instance, is assumed to be a constant system with a single input and output, and the learning rate demonstrates how it impacts everything. Equation (18) can be found by entering all of the terms from equation (17) after they have been calculated. The parameter's updated value has been provided.

a_{A1} :

$$a_{A1}(n+1) = a_{A1}(n) + 2.\eta.\xi(n).f_1(n).\frac{(\overline{\mu_2}(n) + \overline{\mu_3}(n))}{\mu_{A1}(n) + \mu_{A2}(n) + \mu_{A3}(n)}.\frac{\mu_{A1}(n) - 1}{b_{\lambda 1}(n) - a_{\lambda 1}(n)} \quad (23)$$

Similarly

$$b_{A1}(n+1) = b_{A1} - 2.\eta.\xi(n).f_1(n).\frac{(\overline{\mu_2}(n) + \overline{\mu_3}(n))}{\mu_{A1}(n) + \mu_{A2}(n) + \mu_{A3}(n)}.\frac{\mu_{A1}(n)}{b_{\lambda 1}(n) - a_{\lambda 1}(n)} \quad (24)$$

This also generates the precondition parameters that appear as follows for the fuzzy membership functions that are still present:

$$b_{A2}(n+1) = b_{A2} + 2.\eta.\xi(n).f_2(n).\frac{(\overline{\mu_1}(n) + \overline{\mu_3}(n))}{\mu_{A1}(n) + \mu_{A2}(n) + \mu_{A3}(n)}.\frac{1 - \mu_{A2}(n)}{b_{A2}(n)} \quad (25)$$

$$a_{A3}(1+n) = a_{A3}(n) + 2.\eta.\xi(n).f_3(n).\frac{(\overline{\mu_1}(n) + \overline{\mu_2}(n))}{\mu_{A1}(n) + \mu_{A2}(n) + \mu_{A3}(n)}.\frac{\mu_{A3}(n) - 1}{b_{A3}(n) - a_{A3}(n)} \quad (26)$$

$$b_{A3}(n+1) = b_{A3}(n) - 2.\eta.\xi(n).f_3(n).\frac{(\overline{\mu_1}(n) + \overline{\mu_2}(n))}{\mu_{A1}(n) + \mu_{A2}(n) + \mu_{A3}(n)}.\frac{\mu_{A3}(n)}{b_{A3}(n) - a_{A3}(n)} \quad (27)$$

b). **Consequently Adjusting Parameters:** The following revised laws are applied as tuning factors for the subsequent parameters in Layer 4.

$$a_{0_i}(n+1) = a_{0_i}(n) - \eta_c.\frac{\partial \xi^2}{\partial_{a_{0_i}}} \quad i = 1,2,3 \quad (28)$$

$$a_{1_i}(n+1) = a_{1_i}(n) - \eta_c.\frac{\partial \xi^2}{\partial_{a_{1_i}}} \quad i = 1,2,3 \quad (29)$$

For subsequent parameters, the learning rate is represented by η_c. The chain rule can also be used to determine the derivative terms in equations (28)–(29) in the following way

$$\frac{\partial \xi^2}{\partial_{a_{0_i}}} = \frac{\partial \xi^2}{\partial V\_}.\frac{\partial V\_}{\partial i\_}.\frac{\partial i\_}{\partial f_i}.\frac{\partial_{fi}}{\partial_{a_{0_i}}}, \quad i = 1,2,3 \quad (30)$$

$$\frac{\partial \xi^2}{\partial_{a_{1_i}}} = \frac{\partial \xi^2}{\partial V\_}.\frac{\partial V\_}{\partial i\_}.\frac{\partial i\_}{\partial f_i}.\frac{\partial_{fi}}{\partial_{a_{0_i}}}, \quad i = 1,2,3 \quad (31)$$

The final two terms on the root harmonic sum of equations (30)–(31) can be obtained in this way, while the initial two terms are pre-known.

$$\frac{\partial_i}{\partial_{f_i}} = \frac{\mu_i}{\mu_{A1} + \mu_{A2} + \mu_{A3}} \quad i = 1, 2, 3 \quad (32)$$

$$\frac{\partial_{f_i}}{\partial_{a_{0_i}}} = 1 \quad i = 1,2,3 \quad (33)$$

$$\frac{\partial_{f_i}}{\partial_{a_{1_i}}} = \xi, \quad i = 1, 2, 3 \quad (34)$$

Adaptability A neuro deceptive structure known as a flexible neuro-delicate affirmation driving force is based on the Takagi-Sugeno pleasant enrollment composition.

$$a_{o1}(n+1) = a_{o1}(n) + 2.\eta_c.\zeta.\frac{\mu i}{\mu_{A1} + \mu_{A2} + \mu_{A3}}, \quad i=1, 2, 3 \quad (35)$$

$$a_{1i}(n+1) = a_{1i}(n) + 2.\eta_c.\zeta.\frac{\mu i}{\mu_{A1} + \mu_{A2} + \mu_{A3}}.\xi \quad i=1, 2, 3. \quad (36)$$

4 AFPI- Controller

Adaptable neuro-fuzzy inference system, sometimes referred to as a flexible neuro-delicate, is a neuro deceptive structure. affirmation driving force is based on the Takagi-Sugeno pleasant enrollment composition. or versatile structure based warm reasoning system (ANFIS). In the mid-1990s, the framework was created. It can obtain the benefits of both in a single construction since it constructs both neuronal systems and buffered current measures. The enrollment structure of the program takes into account a methodology of cushioning IF-THEN choices, which can learn from incorrect nonlinear cutoff points. Thus, it is acknowledged that ANFIS is a full estimator. The optimal parameters found by inborn calculation can be used to use the ANFIS in a somewhat more precise and profitable manner. Artificial Neuro-Fuzzy Inference Systems is referred to as ANFIS.

1. A type of flexible frameworks known as AFPI is indistinguishable from feathery deducing structures in every practical sense.

2. Sugeno e Tsukamoto cushioning models are covered by AFPI.

3. A mutt is used by AFPI to assist with problem-solving.

Neuro-cushioned deduces blends of distorted brain structures and woolen aid in the realm of motorized thinking. Neuro-comfortable hybridization grasps a cream-colored structure that combines the learning and connectionist structure of neural systems with the human-like thinking style of cushioning structures to create a system that harmonizes these two systems. The word that is most frequently used to describe neuro-cushioned hybridization in the developed work is Fuzzy Neural Network (FNN) or Neuro-Fuzzy System (NFS). The phrase "neuro-cushioned structure," which will be employed henceforth, describes how the human-like thinking style of woolen frameworks is wired using comfortable sets and a semantic model with an IF-THEN cushioned standards approach. The underlying idea behind neuro-fleecy structures is that they are amorphous, which means that no matter how you look at them, their power to pose interpretable IF-THEN questions controls the game. Interpretability and accuracy are two contradictory needs for a comfortable appearance, and the plausibility of neuro-fragile structures unites them. That is the only factor that truly counts; among the two qualities, one is dominant. There are two zones in the neuro-warm cushioned showing exploring field: right fleecy demonstrating that depends upon exactness, generally exemplified by the Takagi-Sugeno-Kang (TSK) portrayal; and semantic sensitive displaying that is based on interpretability, primarily the Mamdani show. Observing multi-layer feed-forward connectionist structures for fuzzification cushioned actuation and defuzzification. It is important to note that the Mamdani-type neuro-comfortable systems may lose their interpretability. Certain assessments, in which crucial components of the interpretability of neuro-comfortable structures are similarly divided, are necessary to improve the interpretability of neuro-cushioned systems. An assessment line that propels itself keeps an eye out for the data stream mining scenario, in which neuro-cushioned structures are progressively given new capabilities to advance toward points of interest in real time. In a similar vein, framework revivals combine not only a recursive variation in model parameters but also a potent progression and pruning of the model with a particular extreme target to manage cognitive float and consistently alter structure lead in a satisfactory manner and to maintain the structures/models "in the present style" at all times.

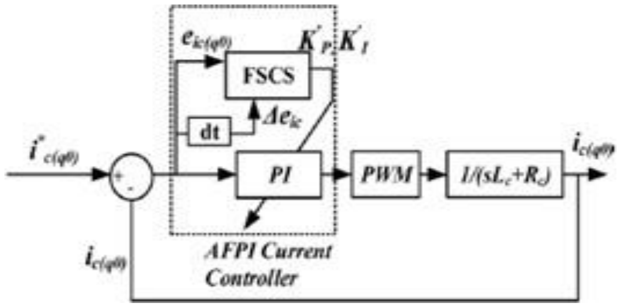

Figure 6: GIC's q_o-axis control diagram with the AFPI Controller

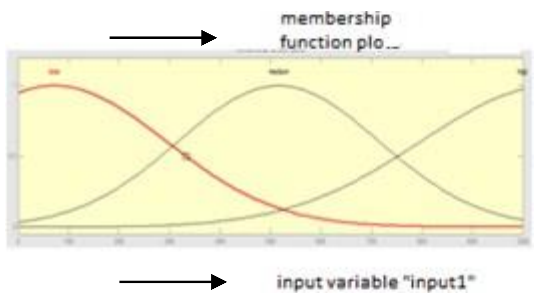

Figure 7: Input Signal 1

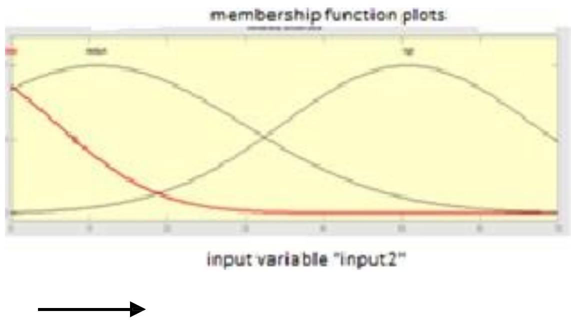

Figure 8: Input Signal 2

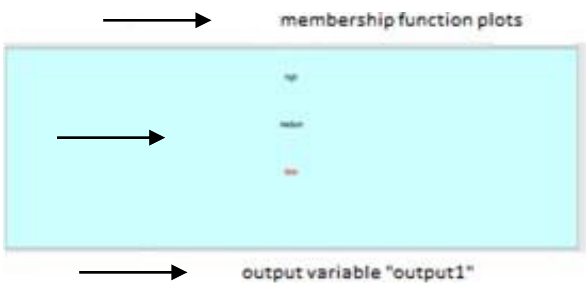

Figure 9: Output Variable

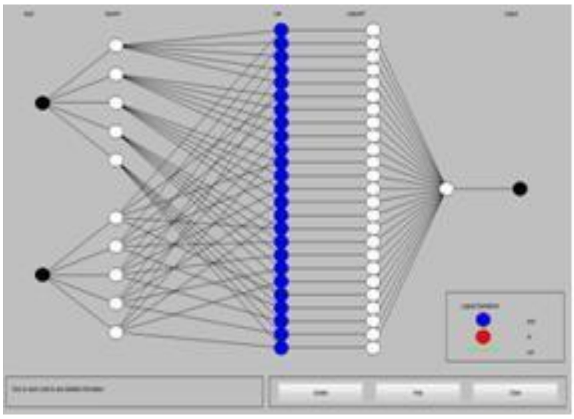

Figure 10: Fuzzily organized

5 Simulation Results

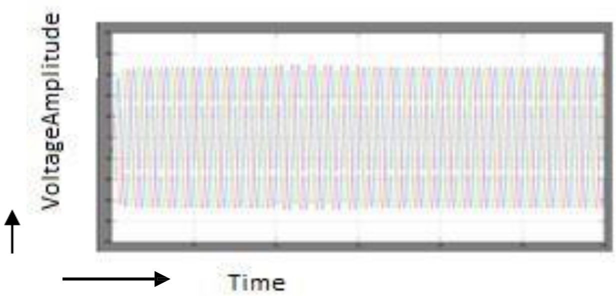

Figure 11: 3 Phase Voltage

Figure 12: Un Balanced Load Current

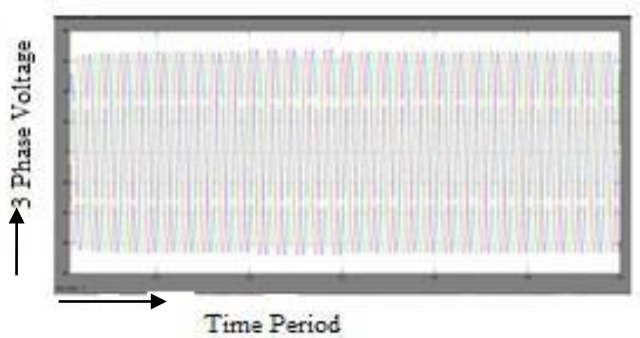

Figure 13: 3 phase Balance Voltage

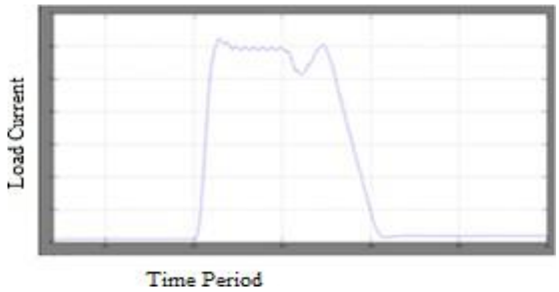

Figure 14: 3 phase Balance Voltage Factor

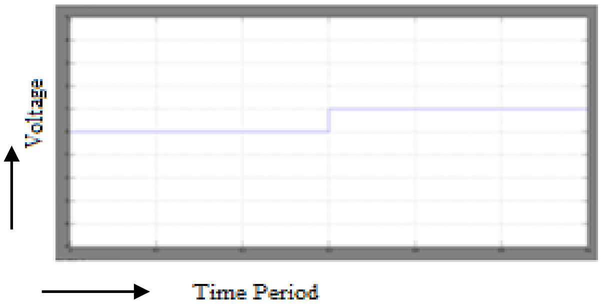

Figure 15: Control Signal

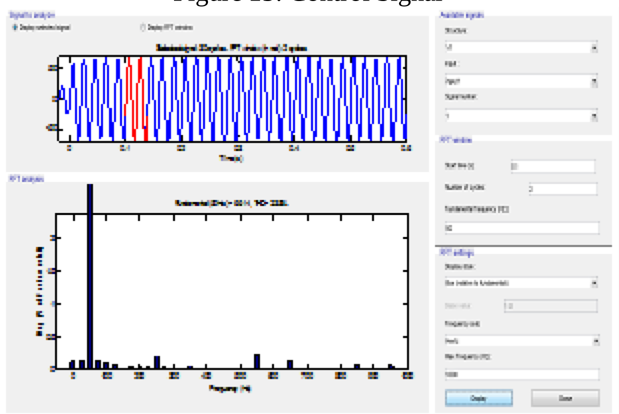

Figure 16: THD

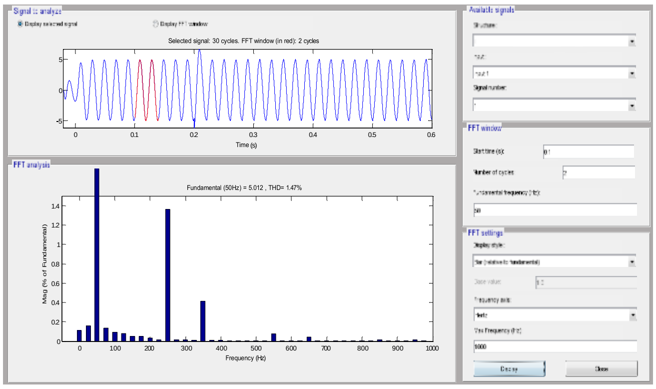

Figure 17: Current Waveform

Simulation Results by using AFPI controller

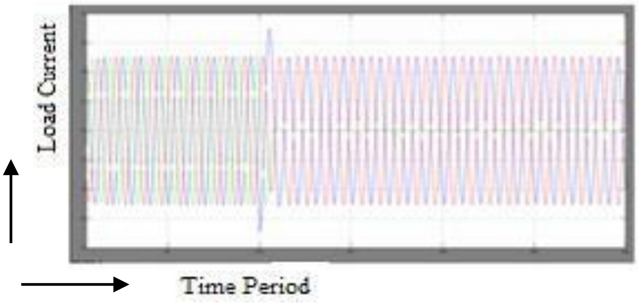

Figure 18: Three Phase Load Current

Figure 19: Control Signal

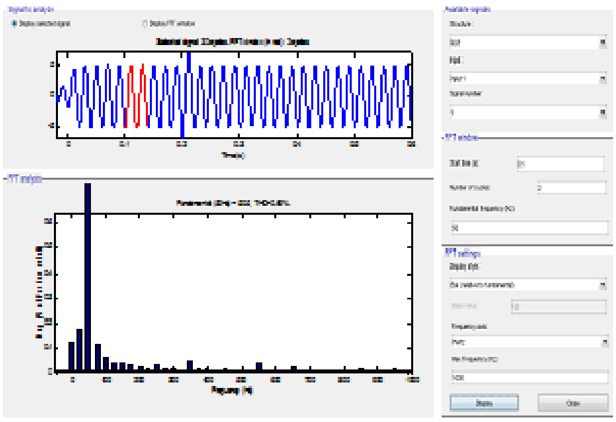

Figure 20: Output Current Waveform

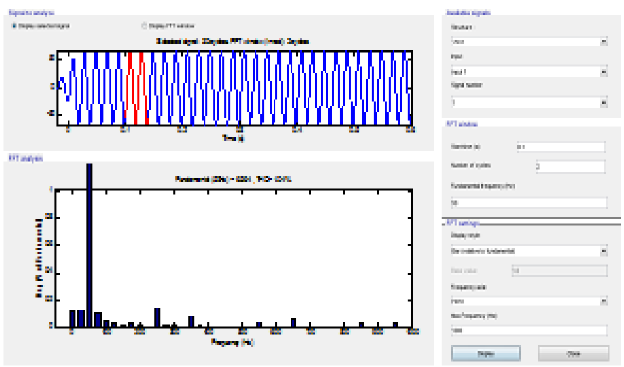

Figure 21: Output Voltage Waveform

6 Conclusion

This publication describes the successful design, simulation, and implementation of an ANFIS-based add-on controller on a scaled hardware prototype in a lab context. In this instance, it has been shown that individual VSCs in a microgrid may be managed so that load disruptions barely affect the voltage profile. In this study, the extreme load unbalance conditions—such as abruptly turning off a phase to create Consideration has been given to a 3-phase balance load that throws off a 2-phase load. Still, the voltage waveform is unaffected by the load's sudden action. The influence of the suggested control algorithm has been validated by presenting and thoroughly discussing the simulation findings backed by the experimental results.

References

[1] J. Rocabert, A. Luna, F. Blaabjerg, and P. Rodrguez, Control of Power Converters in AC Microgrids, IEEE Transactions on Power Electronics, vol. 27, pp. 4734-4749, Nov. 2012.

[2] Y. W. Li, D. M. Vilathgamuwa, and P. C. Loh, A Grid-Interfacing Power Quality Compensator for Three-Phase Three-Wire Microgrid Applications, IEEE Transactions on Power Electronics, vol. 21, pp. 1021-1031, Jul. 2006.

[3] C. Marnay, H. Asano, S. Papathanassiou, and G. Strbac, Policymaking of Micro grids, Economic and regulatory issue of microgrid implementation, IEEE Power \& Energy magazine, May 2008.

[4] B. Sorensen, Renewable Energy, 4th ed. Academic Press, Elsevier, 2011.

[5] Trivedi, D. K. Jain, and M. Singh, A modified droop control method for parallel operation of VSItextquotesingles in microgrid, in 2013 IEEE Innovative Smart Grid Technologies-Asia (ISGT Asia), Nov. 2013.

[6] Trivedi and M. Singh, Repetitive Controller for VSIs in Droop Based AC-Microgrid, IEEE Transactions on Power Electronics, pp. 1-1, 2016.

[7] M. Savaghebi, A. Jalilian, J. C. Vasquez, and J. M. Guerrero, Secondary Control Scheme for Voltage Unbalance Compensation in an Islanded Droop-Controlled Microgrid, IEEE Trans. Smart Grid, vol. 3, pp. 797-807, Jun. 2012.

[8] Hui Li, K. L. Shi, P. G. McLaren, Neural-Network-Based Sensor-less Maximum Wind Energy Capture With Compensated Power Coefficient, IEEE Trans. Ind. Appl., vol. 41, no. 6, pp. 1548-1556, Nov. 2005

[9] M. Singh, and A. Chandra, ANFIS Based Speed & Position Sensor less Control of Grid Connected, PMSG coupled Wind Turbine with 3P4W Non-Linear Unbalance Load Compensation ,.

[10] J. Shing and R. Jang, ANFIS: Adaptive-Network-Based Fuzzy Inference System, IEEE Trans. On Systems, Man, and Cybernetics, vol. 23, no. 3, pp. 665-685, May 1993.

[11] P. Garcia, C.A. Garcia, L.M. Fernandez, F. Llorens and F. Jurado, ANFIS-based Control of a Grid-connected Hybrid System Integrating Renewable Energies, Hydrogen and Batteries,

[12] M. Singh, and A. Chandra, Real Time Implementation of ANFIS Control for Renewable Interfacing Inverter in 3P4W Distribution Network, IEEE Trans. Industrial Electron, vol. 60, no.1, pp. 121-128, Jan. 2013.